Time-Domain Surface Impedance Boundary Conditions Enhanced by Coarse Volume Finite-Element Discretisation

Ruth V. Sabariego[1], Christophe Geuzaine[1], Patrick Dular[1,2] and Johan Gyselinck[3]

[1] Dept. of Electrical Engineering and Computer Science (ACE), University of Liège, Belgium
[2] Fonds de la Recherche Scientifique - F.R.S.-FNRS, Belgium
[3] Dept. of Bio-, Electro- and Mechanical Systems (BEAMS), Université Libre de Bruxelles (ULB), Belgium

In computational magnetodynamics, surface impedance boundary conditions allow to accurately account for high-frequency flux components while removing the massive conducting regions from the computation domain. The time-domain approach previously proposed by the authors relies on the spatial discretisation of a 1-D eddy-current problem by means of dedicated basis functions derived from the analytical frequency-domain solution. In this paper, these time-domain impedance conditions are combined with a coarse volume finite-element discretisation of the massive conductors to capture slowly varying flux components. The accuracy of the hybrid approach can further be improved by introducing a fictitious frequency-dependent conductivity. The method is illustrated and validated by means of 1-D and 2-D test cases in the frequency and time domain.

Index Terms— **Surface-impedance boundary conditions, finite-element methods, magnetodynamics, time-domain analysis**

I. Introduction

SURFACE impedance boundary conditions (SIBCs) are widely applied in frequency-domain eddy-current problems. They provide approximate relations between the electromagnetic fields at the surface of a massive conducting region, so that the latter can be removed from the computational domain and the computational cost is thus greatly reduced. A necessary condition is that at the considered frequency the skin depth is sufficiently smaller than the finite depth or the curvature of the conducting region. Several high-order SIBC approximations, based on complicated asymptotic expansions, deal with surface curvature, corners, edges, see e.g. [1], [2].

The few time-domain (TD) extensions proposed to date are mostly based on Fourier transform techniques [3], [4], [1], some of which also account for saturation [5], [6]. In [6], the authors presented a low-order TD SIBC approach based on the spatial discretisation of a 1-D eddy-current problem by means of dedicated basis functions derived from its analytical frequency-domain solution. The number of additional basis functions depends on a discrete number of frequencies chosen to cover the working frequency band.

In this paper, the frequency range of this low-order TD SIBC technique is extended down to DC by introducing a coarse volume finite element (FE) discretisation of the massive conducting region and two fictitious frequency-dependent conductivities, linked to its volume and boundary. The coarse FE model complements the TD SIBC technique and inherently accounts for both the curvature and the finite depth of the conducting domain. Besides this coarse volume mesh is much easier to generate (and leads to far fewer unknowns) than the mesh required by a brute force approach, where the skin depth needs to be fully resolved (e.g. with a highly anisotropic boundary-layer like mesh). Preliminary results for a basic 1-D geometry were presented in [7]. The hybrid method is herein further developed and validated on a 2-D application.

Manuscript received July 1, 2011. Corresponding author: R. V. Sabariego (e-mail: r.sabariego@ulg.ac.be).

II. 1-D Eddy-Current Problem

Let us consider a magnetodynamic problem in a semi-infinite slab Ω_m ($0 \leq x \leq \infty$), with the flux density $\underline{b}(x,t)$ and the magnetic field $\underline{h}(x,t)$ parallel to the z-axis, and the current density $\underline{j}(x,t)$ and the electric field $\underline{e}(x,t)$ parallel to the y-axis. For linear and isotropic media, the constitutive laws read $\underline{b} = \mu\,\underline{h}$ and $\underline{j} = \sigma\underline{e}$ where the permeability μ (reluctivity $\nu = 1/\mu$) and the conductivity σ are constant scalars. Under these hypotheses, the 1-D problem is governed by [6]:

$$\partial_x^2 a(x,t) \;=\; \sigma\mu\,\partial_t a(x,t)\,, \qquad a(x=\infty,t) = 0\,, \tag{1}$$

with $a(x,t)$ the $y-$component of the magnetic vector potential $\underline{a}$ ($\underline{b} = \mathrm{curl}\,\underline{a}$, $\underline{j} = -\partial_t\underline{a}$). The uniqueness of $a(x,t)$ is ensured via the boundary condition at infinity $x = \infty$.

Using complex notation (symbols in bold, imaginary unit $\boldsymbol{\imath} = \sqrt{-1}$), the sinusoidal steady-state solution of (1) at frequency f (pulsation $\omega = 2\pi f$), with boundary condition $a(x=0,t) = \hat{a}\,\cos(\omega t + \phi)$, can be written as

$$\boldsymbol{a}(x) \;=\; \hat{a}\,e^{\boldsymbol{\imath}\,\phi}\; e^{-\frac{1+\boldsymbol{\imath}}{\delta}\,x}\,, \tag{2}$$

with $\delta = \sqrt{1/(\mu\sigma\pi f)}$ the skin depth and ϕ an arbitrary phase angle. This analytical solution allows us to write the 1-D frequency-domain SIBC, i.e.

$$\partial_x \boldsymbol{a}\Big|_{x=0} \;=\; -\frac{1+\boldsymbol{\imath}}{\delta}\,\boldsymbol{a}(x=0)\,, \tag{3}$$

that relates the tangential components of the electric and magnetic field, $\boldsymbol{e} = -\boldsymbol{\imath}\omega\boldsymbol{a}$, $\boldsymbol{h} = \nu\,\partial_x\boldsymbol{a}$, at the surface $x = 0$ of the conducting region.

More generally, the 3-D classical SIBC impedance reads

$$\boldsymbol{Z} = \frac{1}{\sigma\,\delta}\,\frac{\underline{n}\times(\boldsymbol{h}\times\underline{n})}{\underline{n}\times\boldsymbol{e}}\,, \tag{4}$$

with $\underline{n}$ the outward normal at the boundary. Note that in the case of an infinitely deep conductor, as supposed above, we have $\boldsymbol{Z} = 1/(1+\boldsymbol{\imath})$.

A. Low-order TD SIBC model

Based on the 1-D analytical solution (2), we choose a number of exponentially decreasing trigonometric basis functions that cover the relevant frequency range. A set of n skin depths δ_k (frequencies f_k), $1 \le k \le n$, are preset for the wished accuracy and $2n$ basis functions defined [6]:

$$\alpha_{c1}(x) = e^{-x/\delta_1} \cos(x/\delta_1)\,, \tag{5}$$

$$\alpha_{ck}(x) = e^{-x/\delta_k} \cos(x/\delta_k) - \alpha_{c1}(x)\,, \quad 2 \le k \le n\,, \tag{6}$$

$$\alpha_{sk}(x) = e^{-x/\delta_k} \sin(x/\delta_k)\,, \quad 1 \le k \le n\,. \tag{7}$$

Note that all but the first basis function vanish at the boundary. The FE discretisation of the variational form of (1) by means of $2n$ basis functions $\alpha_i(x)$, $0 \le x < \infty$, $1 \le i \le 2n$, leads to a system of $2n$ first-order differential equations [6]:

$\nu\,[\mathcal{S}][A(t)] + \sigma\,[\mathcal{M}]\,\partial_t[A(t)] = 0$,, with the elements of $[S]$ and $[M]$ given by

$$s_{ij} = \int_0^\infty \partial_x\alpha_i\,\partial_x\alpha_j\,dx\,, \quad m_{ij} = \int_0^\infty \alpha_i\,\alpha_j\,dx\,. \tag{8}$$

A set of frequencies such that $f_{k+1}/f_k = 10$, $k = 1, \cdots, n-1$, yields a good accuracy in the interval $[f_1, f_n]$, as will be shown in the following sections (with $n = 3$ and different values for f_1, see e.g. Fig. 3).

B. FE discretisation versus TD SIBC approach

Let us consider a massive conducting 1-D problem with depth $L = 100\,\text{mm}$ ($0 \le x \le L$), $\mu_r = 1$ and $\sigma = 60\,\text{MS/m}$, which is uniformly meshed, either coarsely or finely ($\Delta x = 5\,\text{mm}$ or $0.125\,\text{mm}$). Frequency domain solutions are considered for the frequency range from 1e-1 to 1e7 Hz with the $\underline{a}-$formulation. Three flux patterns obtained with the FE model are shown in Fig. 1 (2-D representation of the 1-D model, width 6.25 mm).

Fig. 1. 1D FE model and flux patterns at 10 Hz, 100 Hz and 1000 Hz (skin depth equal to 2.05 cm, 0.65 cm and 0.21 cm, respectively).

The complex impedance $\boldsymbol{Z}$, eq. (4), obtained with the two FE discretisations, the classical SIBC and the TD SIBC approach is depicted in Fig. 2. Its real and imaginary parts, $Re(\boldsymbol{Z})$ and $Im(\boldsymbol{Z})$, differ from 1 due to the finite depth L and the discretisation error. With discrete frequencies $f_1 = 1e2$, $f_2 = 1e3$ and $f_3 = 1e4\,(\text{Hz})$, the TD SIBC shows a very good accuracy in the interval $[f_1, f_3]$, i.e. $Re(\boldsymbol{Z})$ and $Im(\boldsymbol{Z})$ close to 1, with some overshoot on both sides. Clearly, the fine and coarse FE models are accurate from 0 Hz up to, say, $1e1$ Hz and $1e5$ Hz, respectively.

Let us consider now different FE discretisations and different intervals for the TD SIBC. The FE models with element size $\Delta x = 10, 5, 2.5, 0.125\,\text{mm}$, are accurate up to, say, $1e1, 1e2, 1e3$ and $1e6$ Hz, respectively (Fig. 3, up). Note in Fig. 3 (down) the shift in frequency of the TD SIBC curves.

The hybrid approach consists in combining the TD SIBC approximation with a coarse volume FE mesh of the massive conducting region for allowing slowly varying flux components. Considering these two flux paths in parallel is equivalent to adding the two respective complex impedances.

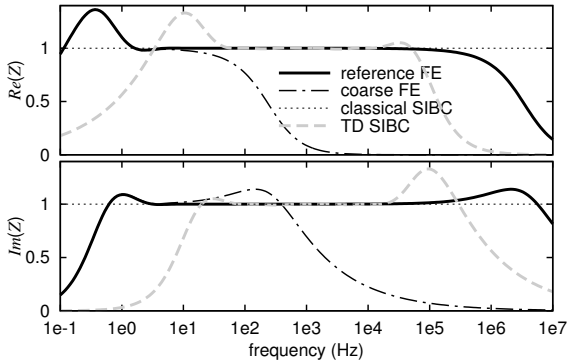

Fig. 2. Real (up) and imaginary (down) parts of the complex impedance $\boldsymbol{Z}$ vs. frequency.

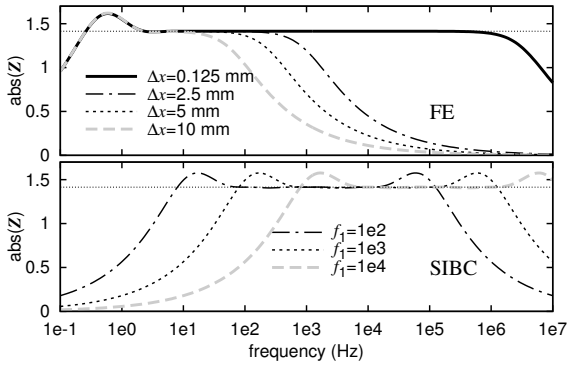

Fig. 3. Modulus of the complex impedance $\boldsymbol{Z}$ vs. frequency obtained with different FE meshes (up) and with TD SIBC approximations (down).

In Fig. 4, the coarse FE model with Δx=5 mm is combined with three different TD SIBC models with $n = 3$. One can observe that for a given FE discretisation, we can find a suitable lowest interval frequency for the TD SIBC, $f_1 = 1e4$, that provides a quite acceptable combination, specially at low and high frequencies.

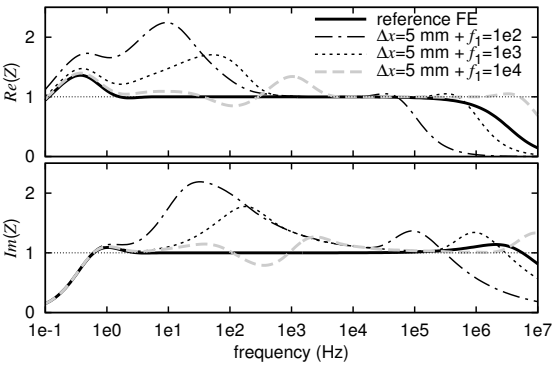

Fig. 4. Real (up) and imaginary (down) parts of the complex impedance $\boldsymbol{Z}$ vs. frequency. The coarse FE model with Δx=5 mm is combined with the TD SIBC approximations in Fig. 3, down.

C. Hybrid approach with frequency dependent conductivity

For further improving the proposed hybrid method, we may increase the slope of the curves $Re(\boldsymbol{Z})$ and $Im(\boldsymbol{Z})$ (see Fig. 2) for both the FE coarse model and the TD SIBC model. With that purpose, we introduce two fictitious frequency-dependent

conductivities to force a quicker drop to zero on the left side of the interval $[f_1, f_n]$. We adopt a conductivity σ^v for the coarse FE volume discretisation and conductivity σ^s for the TD SIBC surface discretisations:

$$\sigma^v = \sigma\Big(1+\sum_{k=1,\dots}(f/c_k)^{2k}\Big), \quad \sigma^s = \sigma\Big(1+\sum_{k=1,\dots}(c'_k/f)^{2k}\Big), \quad (9)$$

with coefficients c_k and c'_k properly fitted for chosen polynomial orders. For the sake of simplicity, polynomial expansions with odd powers are avoided to ensure real conductivity values.

The combination of the coarse FE (with σ^v) and the TD SIBC (with σ^s) in Fig. 5, achieved with the optimised values $c_1 = 12.4, c_2 = 9.1, c_3 = 9.2$ and $c'_1 = 9.4, c'_2 = 10.5, c'_3 = 9.4$ (in Hz), exhibits an excellent agreement with the reference FE $\boldsymbol{Z}$ in the frequency range between 0 and 1e4 Hz.

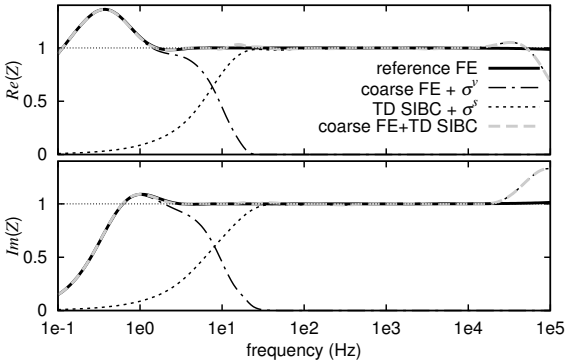

Fig. 5. Real (up) and imaginary (down) parts of the complex impedance $\boldsymbol{Z}$ vs. frequency.

These coefficients c_k and c'_k are fitted by means of a 1-D eddy-current problem with the suitable material characteristics and frequency range of the application at hand for further use in a 2-D or 3-D model.

III. Integration in FE model

Let us consider a 3-D bounded domain $\Omega = \Omega_c \cup \Omega_c^C$ with conducting and non conducting parts Ω_c and Ω_c^C and boundary Γ. The TD SIBC method is applied to a massive sub-domain Ω_m of Ω_c with boundary Γ_m. From the classical $\underline{a}-$ formulation, it reads [6]:

Find $\underline{a}_i$, $i = 0, \cdots, 2n-1$, such that:

$$(\nu\,\mathrm{curl}\,\underline{a}_0, \mathrm{curl}\,\underline{a}'_0)_{\Omega\setminus\Omega_m} + (\sigma\,\partial_t\underline{a}_0, \underline{a}'_0)_{\Omega_c\setminus\Omega_m} - (\underline{j}_s, \underline{a}'_0)_{\Omega_s}$$
$$+ \sum_0^{2n-1}\langle\nu\, s_{i,0}\,\underline{a}_i, \underline{a}'_0\rangle_{\Gamma_m} + \sum_0^{2n-1}\langle\sigma\, m_{i,0}\,\partial_t\underline{a}_i, \underline{a}'_0\rangle_{\Gamma_m} = 0\,,\ \forall\underline{a}'_0\,,$$
$$\sum_0^{2n-1}\langle\nu\, s_{i,j}\,\underline{a}_i, \underline{a}'_j\rangle_{\Gamma_m} + \sum_0^{2n-1}\langle\sigma\, m_{i,j}\,\partial_t\underline{a}_i, \underline{a}'_j\rangle_{\Gamma_m} = 0\,,$$
$$\forall\underline{a}'_j\,, j = 1, \cdots, 2n-1\,, \quad (10)$$

where $(\cdot\,,\cdot)_\Omega$ and $\langle\cdot\,,\cdot\rangle_\Gamma$ are the integrals on the domain Ω and the boundary Γ, respectively, of the product of the two arguments. The scalar values $s_{i,j}$ and $m_{i,j}$ can be pre-calculated by (8). At the discrete level, $\underline{a}_0$ is discretised in $\Omega\setminus\Omega_m$, and $\underline{a}_i$, $i = 1, ..., 2n-1$ are discretised in Γ_m with e.g. Whitney nodal elements.

The hybrid FE–SIBC approach adds unknowns at Γ_m, that are combined with the unknowns in the volume by means of a layer of elements $\Omega_l \subset \Omega_c^C$ that touches Γ_m. The system of coupled equations reads:

Find $\underline{a}_i$, $i = 0, \cdots, 2n$, such that:

$$(\nu\,\mathrm{curl}\,\underline{a}_0, \mathrm{curl}\,\underline{a}'_0)_\Omega + (\sigma\,\partial_t\underline{a}_0, \underline{a}'_0)_{\Omega_c} + (\nu\,\mathrm{curl}\,\underline{a}_1, \mathrm{curl}\,\underline{a}'_0)_{\Omega_l}$$
$$= (\underline{j}_s, \underline{a}'_0)_{\Omega_s}\,, \forall\underline{a}'_0\,,$$
$$(\nu\,\mathrm{curl}\,\underline{a}_0, \mathrm{curl}\,\underline{a}'_1)_{\Omega_l} + (\nu\,\mathrm{curl}\,\underline{a}_1, \mathrm{curl}\,\underline{a}'_1)_{\Omega_l}$$
$$+ \sum_1^{2n}\langle\nu\, s_{i,1}\,\underline{a}_i, \underline{a}'_1\rangle_{\Gamma_m} + \sum_1^{2n}\langle\sigma\, m_{i,1}\,\partial_t\underline{a}_i, \underline{a}'_1\rangle_{\Gamma_m} = 0\,,\ \forall\underline{a}'_1\,,$$
$$\sum_1^{2n}\langle\nu\, s_{i,j}\,\underline{a}_i, \underline{a}'_j\rangle_{\Gamma_m} + \sum_1^{2n}\langle\sigma\, m_{i,j}\,\partial_t\underline{a}_i, \underline{a}'_j\rangle_{\Gamma_m} = 0\,,$$
$$\forall\underline{a}'_j\,, j = 2, \cdots, 2n\,. \quad (11)$$

At the discrete level, $\underline{a}_0$ is discretised in $\bar{\Omega}$, and the $\underline{a}_i$, $i = 1, ..., 2n$ are discretised in Γ_m with Whitney nodal elements.

In the frequency domain, the fictitious conductivities $\sigma^{v,s}$ (9) can be straightforwardly incorporated in (11). In the time domain, we take into account the relation between ∂_t and f, i.e. $\partial_t \rightsquigarrow \imath 2\pi f$:

$$\sigma^v\partial_t\underline{a}_0 = \sigma\Big(\partial_t\underline{a}_0 + \sum_{k=1,2,\cdots}(-1)^k/(2\pi c_k)^{2k}\partial_t^{2k}\underline{a}_0\Big)\,, \quad (12)$$

$$\sigma^s\partial_t\underline{a}_i = \sigma\Big(\partial_t\underline{a}_i + \sum_{k=1,2,\cdots}(-1)^k(2\pi c'_k)^{2k}\partial_t^{-2k}\underline{a}_i\Big)\,, \quad (13)$$

where ∂_t^{2k} and ∂_t^{-2k} denote the $2k$-th derivative and the $2k$-th integration in time, respectively.

IV. Application example

The 2-D application example concerns a conducting cylinder (radius $R = 20$ cm; $\sigma = 60$ MS/m, $\mu_r = 1$) inside an inductor (rectangular cross-section) with imposed current. Only a quarter of the geometry is modelled. The classical FE model with a very fine discretisation of the cylinder near its surface (40 layers of progressively thinner quadrangles, Fig. 6 *right*) provides an accurate reference solution for very small δ/R ratios. When applying SIBC techniques, only the mesh outside the cylinder is effectively considered. The hybrid approach requires an additional coarse volume discretisation. The surface of the cylinder is in all cases discretised with 30 elements of ~ 1 cm (Fig. 6).

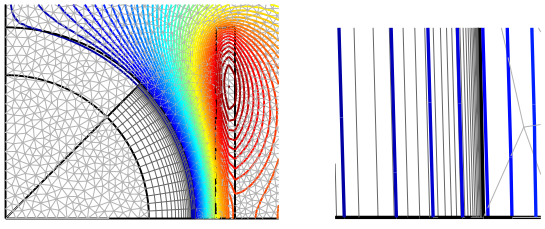

Fig. 6. Flux pattern at 100 Hz, 2-D fine and coarse FE meshes(left). Zoom of mesh near surface (right).

All the approaches have first been compared in the frequency-domain with an imposed sinusoidal current at frequency ranging from 1e-2 to 1e5 Hz. We adopt a low-order approximation of the TD SIBC with $n = 3$, $f_1 = 1e2$ and $f_{k+1}/f_k = 10$. We apply the hybrid approach with optimised frequency-dependent conductivity (Section II-C).

The complex impedance $\boldsymbol{Z}$ (real and imaginary parts) as a function of frequency is shown in Fig. 7, for the reference FE mesh, a coarse mesh, the classical SIBC and TD SIBC approximations, and the hybrid approach. The finite depth and curvature are not taken into account at low frequencies by the classical SIBC are properly captured by the proposed hybrid approach. The inductance of the source (normalised by

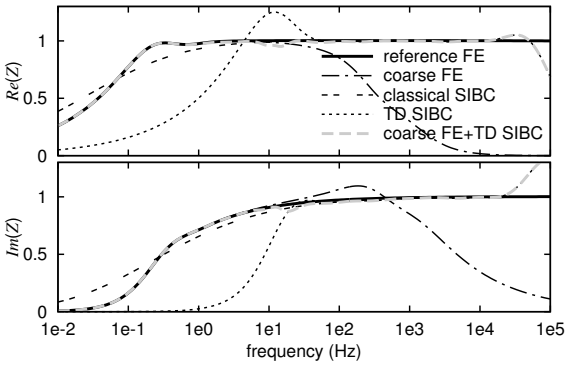

Fig. 7. Real (up) and imaginary (down) parts of the complex impedance $\boldsymbol{Z}$ vs. frequency.

its value at 0 Hz) is shown in Fig. 8. The hybrid approach proves accurate when the classical SIBC, the TD SIBC and the coarse FE are not. The real and imaginary part of the

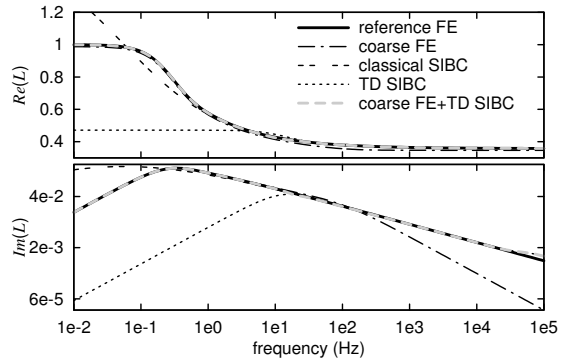

Fig. 8. Real and imaginary part of normalised inductance vs. frequency.

inductance of the source (normalised by its value at 0 Hz) is shown in Fig. 8. The hybrid approach proves accurate when the TD SIBC and the coarse FE are not.

A trapezoidal current varying between 0 and 1 at frequency 100 Hz is next imposed (Fig. 9). A period $T = 1/f = 10$ ms is discretised with a θ-scheme and time step $\Delta t = T/240$. Time-domain results are given for e.g. the fourth period. The flux linkage of the inductor is shown in Fig. 9 for the reference FE model, the TD SIBC and hybrid approaches. While the TD SIBC is not able to capture the DC component, the hybrid approach is. An excellent agreement with the reference FE solution is observed. The magnetic energy and the joule losses in the cylinder are calculated as well and depicted in Fig. 10. A very good agreement between the hybrid and the reference FE results is observed.

V. Conclusion

A low-order time-domain SIBC technique has been combined with a coarse FE discretisation of the massive conducting region in order to capture the slowly varying flux components and accounting for the finite depth and curvature effects. The hybridisation has been further improved by introducing two fictitious conductivities. The effectiveness of the hybrid FE-TD SIBC has been demonstrated with frequency and time-domain results. Further work concerns the study of a real 3-D application.

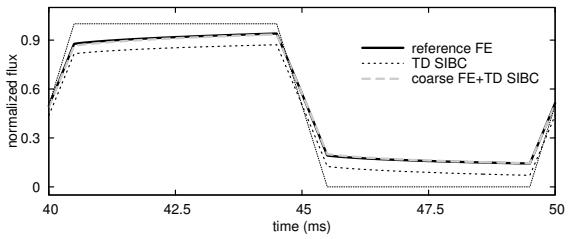

Fig. 9. Normalised magnetic flux vs. time. Trapezoidal imposed current.

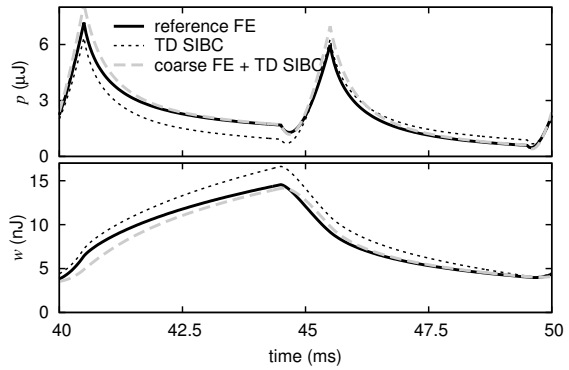

Fig. 10. Joule losses (up) and magnetic energy (down) vs. time.

Acknowledgment

This work has been supported by the Belgian French Community (ARC 09/14-02) and the Belgian Science Policy (IAP P6/21).

References

[1] S. Barmada, L. Di Rienzo, N. Ida and S. Yuferev, "Time domain surface impedance concept for low frequency electromagnetic problems–Part I: Derivation of high order surface impedance boundary conditions in the time domain," *IEE Proc.-Sci. Meas. Technol.*, vol. 152, no. 4, pp. 175–185, 2005.

[2] S. Yuferev and L. Di Rienzo, "Surface impedance boundary conditions in terms of various formalisms," *IEEE Trans. Magn.*, vol. 46, no. 9, pp. 3617–3628, 2010.

[3] K.R. Davey and L. Turner, "Transient eddy current analysis for generalized structures using surface impedances and the fast Fourier transform," *IEEE Trans. Magn.*, vol. 26, no. 3, pp. 1164–1170, 1990.

[4] D. Rodger and H.C. Lai, "A surface impedance method for 3D time transient problems," *IEEE Trans. Magn.*, vol. 35, no. 3, pp. 1369–1371, 1999.

[5] L. Krähenbühl, O. Fabrègue, S. Wanser, M. De Sousa Dias and A. Nicolas, "Surface impedances, BIEM and FEM coupled with 1D non linear solutions to solve 3D high frequency eddy current problems," *IEEE Trans. Magn.*, vol. 33, no. 2, pp. 1167–1172, 1997.

[6] R. V. Sabariego, P. Dular, C. Geuzaine, J. Gyselinck, "Surface-impedance boundary conditions in dual time-domain finite-element formulations," *IEEE Trans. Magn.*, vol. 46, no. 8, pp. 3524–3531, 2010.

[7] J. Gyselinck, P. Dular, C. Geuzaine, and R. V. Sabariego, "Combining surface impedance boundary conditions with volume discretisation in time-domain finite-element modeling," in Proceedings of the 14th Biennial IEEE Conference on Electromagnetic Field Computation (CEFC), Chicago, Illinois, May 9–12, 2010.